World Academy of Science, Engineering and Technology
International Journal of Electronics and Communication Engineering
Vol:1, No:11, 2007

Direction of Arrival Estimation Based on a Single Port Smart Antenna Using MUSIC Algorithm with Periodic Signals

Chen Sun and Nemai Chandra Karmakar

Open Science Index, Electronics and Communication Engineering Vol:1, No:11, 2007 publications.waset.org/8581.pdf

***Abstract*—**A novel direction-of-arrival (DOA) estimation technique, which uses a conventional multiple signal classification (MUSIC) algorithm with periodic signals, is applied to a single RF-port parasitic array antenna for direction finding. Simulation results show that the proposed method gives high resolution (1 degree) DOA estimation in an uncorrelated signal environment. The novelty lies in that the MUSIC algorithm is applied to a simplified antenna configuration. Only one RF port and one analogue-to-digital converter (ADC) are used in this antenna, which features low DC power consumption, low cost, and ease of fabrication. Modifications to the conventional MUSIC algorithm do not bring much additional complexity. The proposed technique is also free from the negative influence by the mutual coupling between elements. Therefore, the technique has great potential to be implemented into the existing wireless mobile communications systems, especially at the power consumption limited mobile terminals, to provide additional position location (PL) services.

***Keywords*—**Direction-of-arrival (DOA) estimation, electronically steerable parasitic array radiator (ESPAR), multiple single classification (MUSIC), position location.

I. Introduction

Over the last few years, there has been an increasing demand for better quality and new value-added services on existing wireless mobile communications networks. This demand has brought technological challenges to service providers. Antennas, so far a neglected component in wireless mobile communications, have gained a renewed interest among researchers. In the form of "smart antennas" or "adaptive array antennas", they meet the challenging demand and bring many benefits to the wireless communications services. These benefits include the enhancement of coverage and the channel capacity, lower transmitted power, better signal quality, higher data rate, and providing value-added services such as users' position location (PL) [1-2]. There are many existing PL systems, such as the Global Position System (GPS), the Global Navigation Satellite System (GLONASS), the Signpost Navigation, and the Cellular Geolocation [3]. The Cellular Geolocation is mainly based on three techniques [4]: the beacon location method, direction-of-arrival (DOA) estimation techniques, and time-difference-of-arrival (TDOA) techniques.

In this paper, we focus on the DOA estimation. Various DOA finding algorithms include conventional methods, linear prediction methods, eigenstructure methods, and estimation of signal parameters via rotational invariance techniques (ESPRIT) [5]. All these methods are based on the digital beamforming (DBF) antenna arrays. Signals, received by individual antenna elements, are down-converted to baseband signals. Then, they are digitized and fed into a digital signal processing (DSP) chip where the DOA estimation algorithm is executed. However, RF circuit branches connected to array elements, analogue-to-digital converters (ADCs) and the baseband DSP chip consume a considerable amount of DC power. Furthermore, each channel connected to the array sensor has the same structure, so the cost of fabrication increases with the number of array elements [6]. All these factors make DBF antenna arrays unsuitable for low power and low cost systems and thus hinder the mass implementation of smart antennas for PL services.

To circumvent these problems of DBF arrays, we propose a novel DOA estimation technique based on a single RF port smart antenna. It is a parasitic array antenna [7], where one central element, connected to the sole RF port, and a number of surrounding parasitic elements form the array. Since the system has only one RF port and one consequent down conversion circuitry, it obviously consumes much less power than a DBF array. Beam steering of parasitic array antennas, by either selecting different sets of parasitic elements with the switching control circuitry in a manner similar to switched beam antennas (called "switched parasitic antennas" [7-11]), or by controlling the reactive loading at the parasitic elements to steer the beam continuously (called "reactively controlled directive arrays" [12] or "aerial beamforming (ABF)" [13-17], shown in Fig. 1), have been extensively studied. However, DOA estimation techniques are only confined to low-resolution estimation

Manuscript received May 14, 2004. This work was mainly done while the authors were with the School of Electrical and Electronic Engineering, Nanyang Technological University, Singapore. This work was supported in part by the National Institute of Information and Communications Technology (NICT) of Japan.

C. Sun was with the School of Electrical and Electronic Engineering, Nanyang Technological University, Singapore. He is now with the ATR Wave Engineering Laboratories, 2-2-2 Hikaridai, "Keihanna Science City", Seika-cho, Soraku-gun, Kyoto, Japan 6190288 (Tel: +81-774-95-2730; fax: +81-774-95-1505; e-mail: sun@ atr.jp).

N. C. Karmakar was with the School of Electrical and Electronic Engineering, Nanyang Technological University, Singapore. He is now with Department of Electrical and Computer Systems Engineering, Monash university, BLDG 72 PO Box 59, Clayton campus, VIC 3800, Australia.

Open Science Index, Electronics and Communication Engineering Vol:1, No:11, 2007 publications.waset.org/8581.pdf

based upon signal powers received from different directions [13]. No such work has been done to explore the eigenstructure based high-resolution technique.

The proposed direction finding technique is based on a reactively controlled directive array [12] structure and utilizes the MUSIC algorithm with periodic signals to explore the signal spatial information. Mobile terminals are required to transmit periodic signals for locating their positions by base stations. The beam pattern is shifted with a predefined angle. So, for the application of MUSIC, it is sufficient to know these angular shifts, without knowing exactly the response to one subset. This is similar to a uniform circular or linear antenna array in which we know the phase shift between consecutive antenna responses, without having to know those responses exactly. The MUSIC algorithm is carried out with the constructed signal vector over 1 period and the modified steering vector based on the beam pattern angle shift. Simulations show that the technique produces a high-resolution DOA estimation in an uncorrelated signal environment, and is feasible to be implemented into practice.

The paper is organized as follows: Section II presents the configuration and the working principle of the reactively controlled directive array. The algorithm for DOA estimation is presented in section III. Results are produced in Section IV, followed by conclusions and recommendations in section V.

II. Design of the Antenna

Figure 2 shows one typical structure of a reactively controlled directive array antenna, called electronically steerable parasitic array radiator (ESPAR) [6]. There, one active central element (monopole) is surrounded by parasitic elements on a circle of radius R on the circular grounded baseplate. The length of each monopole L and the radius R are one-quarter wavelength λ of the transmitting RF signal. The baseplate transforms monopoles with their images to dipoles with a length of 2L. The central monopole is connected to a RF receiver and each parasitic monopole is loaded with a tunable reactor.

The working principle of an ESPAR antenna is different from that for a DBF. The antenna generates a directional beam based on tuning load reactances (x_1, x_2, …, x_6) on the parasitic monopoles. Signals, which are received or transmitted from the central RF port, excite passive monopoles with substantial induced mutual currents on them. In the following discussion, we assume that the antenna works in transmitting mode. Vectors $\mathbf{i}$ and $\mathbf{v}$ represent the current and the voltage on the monopoles, respectively.

$$\mathrm{i} = [i_0 \; i_1 \; i_2 \; i_3 \; i_4 \; i_5 \; i_6]^T , \tag{1}$$

$$\mathbf{v} = [v_0 \; v_1 \; v_2 \; v_3 \; v_4 \; v_5 \; v_6]^T . \tag{2}$$

Superscript T represents the transpose. Mutual admittances are represented by the matrix $\mathbf{Y}$ with each entity y_{ij} denoting for mutual admittance between two elements [15]. There, induced mutual currents are represented by mutual admittances as:

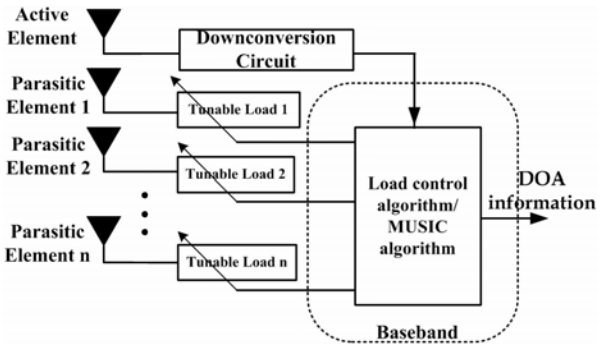

Fig. 1. Functional block diagram of reactively controlled directive arrays [12].

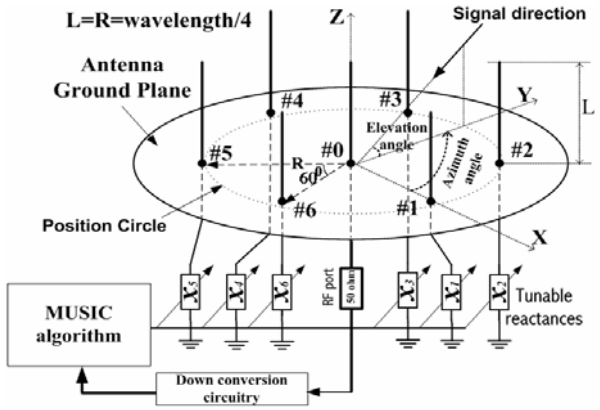

Fig. 2. Configuration of a 7-element ESPAR Antenna [6].

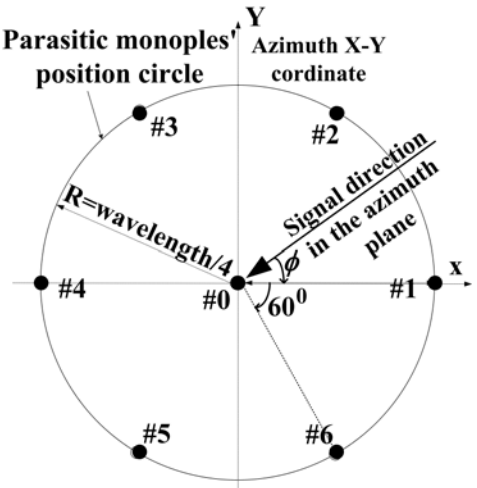

Fig. 3. Geometry of a 7-element ESPAR Antenna.

$$\mathbf{i} = \mathbf{Y}\mathbf{v} = \begin{bmatrix} y_{00} & y_{01} & y_{02} & y_{03} & y_{04} & y_{05} & y_{06} \\ y_{10} & y_{11} & y_{12} & y_{13} & y_{14} & y_{15} & y_{16} \\ y_{20} & y_{21} & y_{22} & y_{23} & y_{24} & y_{25} & y_{26} \\ y_{30} & y_{31} & y_{32} & y_{33} & y_{34} & y_{35} & y_{36} \\ y_{40} & y_{41} & y_{42} & y_{43} & y_{44} & y_{45} & y_{46} \\ y_{50} & y_{51} & y_{52} & y_{53} & y_{54} & y_{55} & y_{56} \\ y_{60} & y_{61} & y_{62} & y_{63} & y_{64} & y_{65} & y_{66} \end{bmatrix} \times \begin{bmatrix} v_0 \\ v_1 \\ v_2 \\ v_3 \\ v_4 \\ v_5 \\ v_6 \end{bmatrix}. \quad (3)$$

For the active central element, the voltages at monopoles are expressed as:

$$v_0 = v_s - z_0 i_0 , \quad (4)$$

where, $z_0 = 50\,\Omega$ is the impedance at the RF port. For parasitic elements $l = 1, \ldots, 6$,

$$v_l = -jx_l i_l , \quad (5)$$

where v_s represents the transmitted voltage signal source, with the amplitude and the phase, from the driving RF port at the central element #0. Represent (4) and (5) with a matrix form:

$$\mathbf{v} = \begin{bmatrix} v_s & 0 & 0 & 0 & 0 & 0 \end{bmatrix}^T - \mathbf{X}\mathbf{i} = v_s \mathbf{u}_1 - \mathbf{X}\mathbf{i} , \quad (6)$$

and define

$$\mathbf{X} = \mathrm{diag}\begin{bmatrix} 50, & jx_1, & \ldots, & jx_6 \end{bmatrix}, \quad (7)$$

$$\mathbf{u}_1 = \begin{bmatrix} 1 & 0 & 0 & 0 & 0 & 0 & 0 \end{bmatrix}^T . \quad (8)$$

Combining (3) and (6), we get:

$$\mathbf{i} = \mathbf{Y}\mathbf{v} = \mathbf{Y}(v_s \mathbf{u}_1 - \mathbf{X}\mathbf{i}) . \quad (9)$$

After a simple mathematical manipulation,

$$\mathbf{i} = v_s (\mathbf{I}_{(7)} + \mathbf{Y}\mathbf{X})^{-1} \mathbf{Y}\mathbf{u}_1 = v_s \mathbf{E}_1 , \quad (10)$$

where matrix $(\mathbf{I}_{(7)} + \mathbf{Y}\mathbf{X})^{-1}\mathbf{Y}\mathbf{u}_1$ is represented as $\mathbf{E}_1$. $\mathbf{I}_{(7)}$ is a 7×7 dimensional identity matrix. The far-field radiation pattern is formed by the superposition of radiation patterns of all monopoles on the antenna ground plane [7, 18]. The far-field current signal, with its amplitude and the phase, in direction ϕ_k is

$$y_{far}(t) = \alpha(\phi_k)\mathbf{i} = v_s \alpha(\phi_k)\mathbf{E}_1 . \quad (11)$$

Assume signals coming in the azimuth plane. The subscript k is the signal sources' index.

$$\alpha(\phi_k) = \begin{bmatrix} 1 & e_1(\phi_k) & e_2(\phi_k) & e_3(\phi_k) & e_4(\phi_k) & e_5(\phi_k) & e_6(\phi_k) \end{bmatrix} . \quad (12)$$

$\alpha(\phi_k)$ is the steering vector corresponding to signal's direction and ϕ_k is given based on the ESPAR antenna geometry (cf. Fig. 3).

$$e_i(\phi_k) = \exp\left\{ j\frac{2\pi}{\lambda} R\cos(\phi_k - \frac{2\pi}{6}(i-1)) \right\} = \exp\left\{ j\frac{\pi}{2}\cos(\phi_k - \frac{\pi}{3}(i-1)) \right\} , \quad \text{for } i = 1, \ldots, 6. \quad (13)$$

Setting the value of v_s in (11) as unity, we can get the array factor $\hat{\alpha}(\phi_k)$ of an ESPAR antenna as:

$$\hat{\alpha}(\phi_k) = \alpha(\phi_k)\mathbf{E}_1 . \quad (14)$$

Thus, the far-field signal in (11) can be represented as

$$y_{far}(t) = \hat{\alpha}(\phi_k) v_s . \quad (15)$$

According to the reciprocity theory for radiation patterns [19], in receiving mode, the received voltage signal $u(t)$ at the RF port is:

$$u(t) = \hat{\alpha}(\phi_k) s_k(t) + n(t) , \quad (16)$$

where, $s_k(t)$ represents kth far-field incident current waves with the amplitude and the phase in the azimuth plane. $n(t)$ is the additive white Gaussian noise (AWGN) with the power of σ^2. When there are totally K impinging waves, the output signals from the RF port are represented as:

$$u(t) = \sum_{k=1}^{K} \hat{\alpha}(\phi_k) s_k(t) + n(t) . \quad (17)$$

Since the $\hat{\alpha}(\phi_k)$ is dependant on the reactance matrix $\mathbf{X}$, antenna beam patterns can be formed in desired directions with nulls in interferers' directions by adjusting reactance values. In practice, the variable reactance is realized by changing the bias voltage of Schottky [20] or varactor diodes loaded at parasitic monopoles.

Based on the previously explained theory, adaptive beamforming algorithms for the ESPAR antenna have been designed [15-17]. In our proposed DOA estimation technique, the ESPAR antenna is not used for adaptive beamforming, though it still has the ability to do so. Here, the antenna is employed to fulfill direction finding. Desired beam patterns are formed to explore the spatial information of the signal sources.

Open Science Index, Electronics and Communication Engineering Vol:1, No:11, 2007 publications.waset.org/8581.pdf

TABLE I. LOAD REACTANCE IN EACH *SAMPLING PERIOD* (#1 TO #6) WHILE THE ANTENNA IS VIRTUALLY ROTATING CLOCKWISE.

Sampling Periods	Values of Load Reactances					
	#1	#2	#3	#4	#5	#6
#1	jX_1	jX_2	jX_3	jX_4	jX_5	jX_6
#2	jX_2	jX_3	jX_4	jX_5	jX_6	jX_1
#3	jX_3	jX_4	jX_5	jX_6	jX_1	jX_2
#4	jX_4	jX_5	jX_6	jX_1	jX_2	jX_3
#5	jX_5	jX_6	jX_1	jX_2	jX_3	jX_4
#6	jX_6	jX_1	jX_2	jX_3	jX_4	jX_5

Open Science Index, Electronics and Communication Engineering Vol:1, No:11, 2007 publications.waset.org/8581.pdf

III. FORMING CORRELATION MATRIX FROM A SINGLE PORT SMART ANTENNA

The MUSIC algorithm, proposed by Schmidt [21], is a relatively simple and high-resolution eigenstructure approach. It has been widely used as a model-based approach for finding the parameters of interest in direction finding or source location problems. There are many improved forms of the MUSIC algorithm, such as: the Root-MUSIC Algorithm, and the beamspace-MUSIC Algorithm [5]. All these algorithms require the snapshots of signals from antenna array elements to form the signal correlation matrix.

It is obvious that we can't apply the conventional MUSIC algorithm to an ESPAR antenna, because it needs groups of signal samples from linear or circular array elements to form a vector; whereas ESPAR antenna has only one RF port, forming signal sample vector is impossible at one time. This is the distinction between the MUSIC algorithm based on a single port smart antenna and the conventional MUSIC algorithm based on a DBF array antennas as aforementioned. However, we can see from the explanation in the following part that received signals from an ESPAR antenna RF port contain signal sources' direction information. The signal correlation matrix can still be formed.

In operation, the antenna is virtually rotated by forming beams with changing the sequence of load reactances in six sampling periods. (cf. Table I) The sample signal vector $\mathbf{u}(t) = [u_1(t)\ u_2(t)\ u_3(t)\ u_4(t)\ u_5(t)\ u_6(t)]^T$ is constructed with signal samples from the RF output. Each entity $u_m(t)$ (m = 1, … , 6) is obtained in the sampling period #m consecutively. The maximum number of sampling periods M = 6 equals the number of the parasitic elements. For an ESPAR antenna with 6 parasitic elements, rotating 6+1 times returns to the original status. Load reactance values of parasitic monopoles are the same for all the sampling periods. E1, defined in (10), remains constant as the antenna rotates virtually. However, signal directions with respect to antenna azimuth place X-Y coordinate change. According to (17), the received signal samples at each sampling period #m are represented as:

$$u_m(t) = \sum_{k=1}^{K} \hat{\alpha}\left(\phi_k - \frac{2\pi}{M}(m-1)\right) s_k(t) + n_m(t) \qquad m = 1, 2, \ldots, 6. \tag{18}$$

For the simplicity we define:

$$\hat{\alpha}_m(\phi_k) = \hat{\alpha}\left(\phi_k - \frac{2\pi}{M}(m-1)\right). \tag{19}$$

$\hat{\alpha}_m(\phi_k)$ contains the kth signal source direction information ϕ_k. $n_m(t)$ is the noise component at the mth sampling period. Suppose that each individual signal source transmits periodic signals, and the length of one signal period is the same as one sampling period. Received signal samples are the same for all sampling periods. Therefore, the received signal vector **u**(t) after six sampling periods is written into the following matrix multiplication equation form:

$$\mathbf{u}(t) = \begin{bmatrix} u_1(t) \\ u_2(t) \\ u_3(t) \\ u_4(t) \\ u_5(t) \\ u_6(t) \end{bmatrix} = \begin{bmatrix} \hat{\alpha}_1(\phi_1) & \hat{\alpha}_1(\phi_2) & \cdots & \hat{\alpha}_1(\phi_k) \\ \hat{\alpha}_2(\phi_1) & \hat{\alpha}_2(\phi_2) & \cdots & \hat{\alpha}_2(\phi_k) \\ \hat{\alpha}_3(\phi_1) & \hat{\alpha}_3(\phi_2) & \cdots & \hat{\alpha}_3(\phi_k) \\ \hat{\alpha}_4(\phi_1) & \hat{\alpha}_4(\phi_2) & \cdots & \hat{\alpha}_4(\phi_k) \\ \hat{\alpha}_5(\phi_1) & \hat{\alpha}_5(\phi_2) & \cdots & \hat{\alpha}_5(\phi_k) \\ \hat{\alpha}_6(\phi_1) & \hat{\alpha}_6(\phi_2) & \cdots & \hat{\alpha}_6(\phi_k) \end{bmatrix} \times \begin{bmatrix} s_1(t) \\ s_2(t) \\ \bullet \\ \bullet \\ \bullet \\ s_k(t) \end{bmatrix} + \begin{bmatrix} n_1(t) \\ n_2(t) \\ \bullet \\ \bullet \\ \bullet \\ n_6(t) \end{bmatrix}. \tag{20}$$

Equation (20) has the same form as the output from an array antenna with 6 elements. In the first matrix of the right-hand side of equation, we define each column as vector $\vec{\alpha}(\phi_k)$. It corresponds to the steering vector [22] for a 6-element array antenna as in array signal processing literature. But each entity is not a phase delay of a source signal at each antenna sensor, induced by the angle of arrival of the plane waves with respect to the array antenna in the azimuth plane. We call $\vec{\alpha}(\phi_k)$ as "ESPAR-Direction Vector" to differentiate it from the term "steering vector" in array processing literatures. The signal correlation matrix at the antenna output is R_{UU}.

Open Science Index, Electronics and Communication Engineering Vol:1, No:11, 2007 publications.waset.org/8581.pdf

$$\mathrm{R}_{\mathrm{UU}} = E(\mathbf{u}(t)\mathbf{u}^{H}(t)) = \frac{1}{Ns}\mathbf{U}\mathbf{U}^{H}. \quad (21)$$

$E(\bullet)$ is the expected value operator. U without time argument represents the discrete samples with sample block length *Ns*. Superscript *H* denotes conjugate-transpose. Suppose all the noise components $n_m(t)$ (m = 1, …, 6) at each sampling period #m are independent and identically distributed (i.i.d.) AWGN with the power of σ^2. R_{UU} is represented as

$$\mathbf{R}_{UU} = \left[\vec{\alpha}(\phi_1)\ \vec{\alpha}(\phi_2) \ldots \vec{\alpha}(\phi_k)\right] \times \mathbf{R}_{SS} \times \left[\vec{\alpha}(\phi_1)\ \vec{\alpha}(\phi_2) \ldots \vec{\alpha}(\phi_k)\right]^{H} + \sigma^2 \mathbf{I}_{(6)}. \quad (22)$$

$\mathrm{I}_{(6)}$ is a 6×6 dimensional identity matrix. The source signal correlation matrix $\mathbf{R}_{SS}$ is

$$\mathbf{R}_{SS} = E\left(\left[s_1(t)\, s_2(t) \cdots s_k(t)\right]^{T} \times \left[s_1(t)\, s_2(t) \cdots s_k(t)\right]^{*}\right), \quad (23)$$

where superscripts *T* and * are transpose and complex-conjugate, respectively. Based on (21), MUSIC algorithm is executed in a similar procedure as the conventional MUSIC algorithm. (cf. Fig. 4) The ESPAR-Direction Vector is used to evaluate the MUSIC spectrum. The algorithm requires signals to be periodic. That means proposed technique cannot be applied when mobile terminals are transmitting message signals, because message signals are quite indeterministic. It can, however, be implemented in a pilot or command channel or by assigning periodic codes at message channels. Therefore, we call it MUSIC algorithm with periodic signals. Its procedure is given below:

1) Construct the signal sample vector given by $\mathbf{u}(t) = [u_1(t)\ u_2(t)\ u_3(t)\ u_4(t)\ u_5(t)\ u_6(t)]^T$, where $u_m(t)$, m = 1, …, 6, is the signal sample when the antenna is at sampling period #m. Finally, form the signal correlation matrix $\mathbf{R}_{\mathrm{UU}}$.
2) Eigendecompose the signal correlation matrix $\mathbf{R}_{\mathrm{UU}}$, and form the noise subspace $\mathbf{E}_N$ with eigenvectors corresponding to the small eigenvalues.
3) Evaluate the MUSIC spectrum PMU versus the signal direction ϕ.

$$P_{MU} = \frac{1}{\left|\mathbf{E}_N{}^{H}\, \vec{\alpha}(\phi)\right|^2} \quad (24)$$

4) $\vec{\alpha}(\phi)$ is the ESPAR-Direction Vector corresponding to the azimuthal looking direction ϕ.
5) Finally, extract impinging waves' direction information.

We can see that besides the additional procedure of forming the signal sample vector, proposed technique has the same procedure as that for the conventional MUSIC algorithm. An extra amount of time is required for saving data to form the signal sample vector.

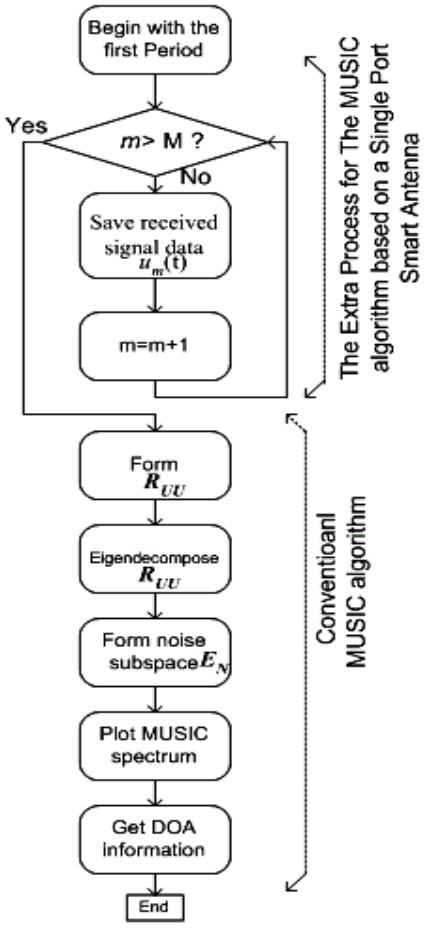

Fig. 4. Flowchart of the MUSIC algorithm and the proposed MUSIC algorithm based on a single port smart antenna.

IV. Simulation

In our simulation, three directional binary phase shift keying (BPSK) signals with the equal power levels are randomly generated. Signal directions are set arbitrarily 120°, 150° and 300° in the azimuth plane, respectively. During each of the six antenna sampling periods, 16 bit signal samples are stored for further processing. This indicates that *Ns* is 16 in (21).

The monopoles on the ground plane of the ESPAR antenna are oriented vertically. Impinging signals are assumed co-polarized with the ESPAR antenna. Cross-polarization coupling typically produced by scatters and reflectors in the multipath propagation environment [23] is not considered.

A. Influence of Parasitic Load Reactance

We study four different reactance load settings to investigate their influence on the performance of DOA estimation. Table II summarizes the reactance values for these four cases. MUSIC spectra with different reactive load settings in uncorrelated signal environments with a signal-to-noise-ratio (SNR) of 30 dB for each individual signal source are presented and explained as follows.

Open Science Index, Electronics and Communication Engineering Vol:1, No:11, 2007 publications.waset.org/8581.pdf

TABLE II. SETTING OF SIX PARASITIC LOADS AT ANY SAMPLING PERIOD. ONCE THE SETTING IS DECIDED, THESE VALUES DO NOT CHANGE DURING THE PROCESS OF DOA ESTIMATION. THE ASSIGNMENT OF THE LOADING CHANGES AS INDICATED IN TABLE I TO ROTATE THE ANTENNA.

Case	x_1 Ω	x_2 Ω	x_3 Ω	x_4 Ω	x_5 Ω	x_6 Ω	MUSIC Spectrum	DOA information
1	30	30	30	30	30	30	Fig. 6	Not shown in the spectrum
2	0	30	0	30	0	30	Fig. 7	Not shown in the spectrum
3	0	30	0	30	30	30	Fig. 9	Shown in the spectrum
4	0	10	0	-30	70	30	Fig. 9	Shown in the spectrum

1) Case 1. Equal Load Reactance of 30 Ω

In Case 1, we set all the parasitic load reactances to 30 Ω. In this case, the antenna exhibits a nearly omnidirectional beam pattern as shown in Fig. 5. Antenna can not be virtually rotated in a way as described before. The MUSIC Spectrum is plotted in Fig. 6. From the figure we can observe, that the information of signal direction can not be extracted.

2) Case 2. Ordered But Unequal Load Reactances of 0 Ω and 30 Ω

In Case 2, we set the load to $x_1 = 0$ Ω, $x_2 = 30$ Ω, $x_3 = 0$ Ω, $x_4 = 30$ Ω, $x_5 = 0$ Ω, $x_6 = 30$ Ω. Two possible beam patterns (Case2_1 & Case2_2) for rotation with this load setting are shown in Fig. 5. The MUSIC spectrum is plotted in Fig. 7. It also cannot give the direction information. From the simulation studies in Cases 1 and 2, we conclude that we should not set the loads "ordered", which will result in insufficient beam patterns for rotation.

3) Case 3. Random Load Reactances of 0 Ω and 30 Ω

In Case 3, we arbitrarily set $x_1 = 0$ Ω, $x_2 = 30$ Ω, $x_3 = 0$ Ω, $x_4 = 30$ Ω, $x_5 = 30$ Ω, $x_6 = 30$ Ω. Six beam patterns (a) to (f) for antenna sampling period #1 to #6 are shown in Fig. 8. Signals' DOA information is clearly indicated in the MUSIC spectrum in Fig. 9.

4) Case 4. Random Load Reactances

Finally, we randomly set the reactance values to: $x_1 = 0$ Ω, $x_2 = 10$ Ω, $x_3 = 0$ Ω, $x_4 = -30$ Ω, $x_5 = 70$ Ω, $x_6 = 30$ Ω. The MUSIC spectrum is plotted in Fig. 9. From the figure, we can see that if the reactance is not set ordered, they only slightly influence the MUSIC spectrum not the performance. All the spectra reach the peak values at signal directions. The beam pattern for this case is shown in Fig. 10. Note that the proposed technique is used for DOA estimation not for beam forming. So the beam pattern does not necessarily correspond to the directions of signals.

From the above investigation, we conclude that the manner of load settings greatly influences algorithm's DOAs estimation performance. When setting the reactive loads, we should avoid setting them ordered. Rather, we set their values arbitrarily to precisely estimate the DOA information. With a symmetric pattern, signals impinging from different directions may produce the same output at the RF port. Analogous to linear array antenna, image peaks appear. Rather, we can set the reactance values arbitrarily to precisely estimate the DOA information.

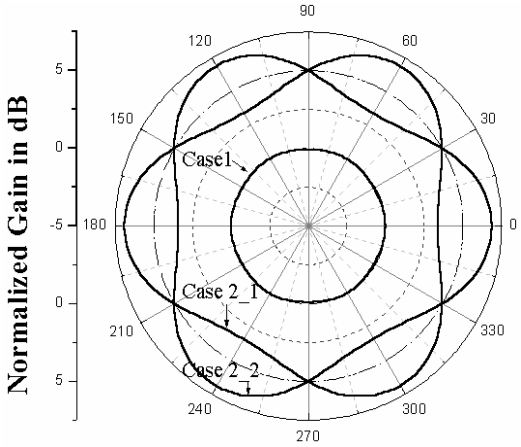

Fig. 5 Beam Pattern for Case 1 (Equal load reactance of 30Ω) and Two Possible Beam Patterns in Case 2 ($x_1 = 0$ Ω, $x_2 = 30$ Ω, $x_3 = 0$ Ω, $x_4 = 30$ Ω, $x_5 = 0$ Ω, $x_6 = 30$ Ω) Are Show with Dot Lines (Case2_1 & Case2_2).

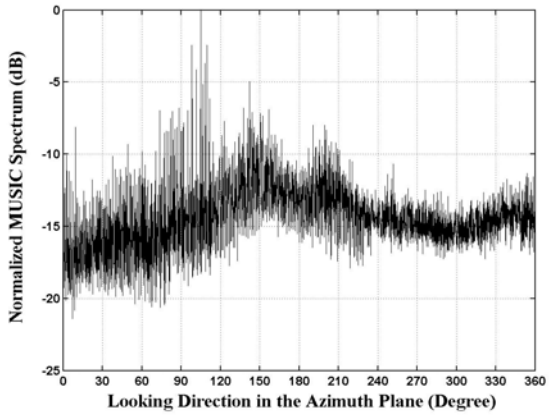

Fig. 6. MUSIC Spectrum for Case 1: $x_l = 30$ Ω ($l = 1,\ldots,6$), SNR = 30 dB and Signal Directions are 120°, 150° and 300° in the Azimuth Plane.

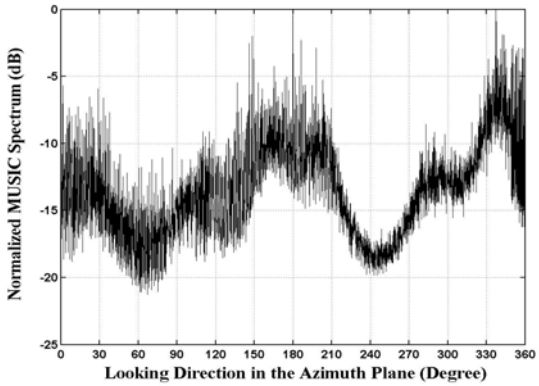

Fig. 7. MUSIC Spectrum for Case 2: $x_1 = 0$ Ω, $x_2 = 30$ Ω, $x_3 = 0$ Ω, $x_4 = 30$ Ω, $x_5 = 0$ Ω, $x_6 = 30$ Ω. SNR = 40 dB. Signal Directions: 120°, 150° and 300° in the Azimuth Plane.

Forming directive beam patterns is not important to the performance. The technique is dependent of the angular shifting of the beam pattern. If only the pattern is not

Open Science Index, Electronics and Communication Engineering Vol:1, No:11, 2007 publications.waset.org/8581.pdf

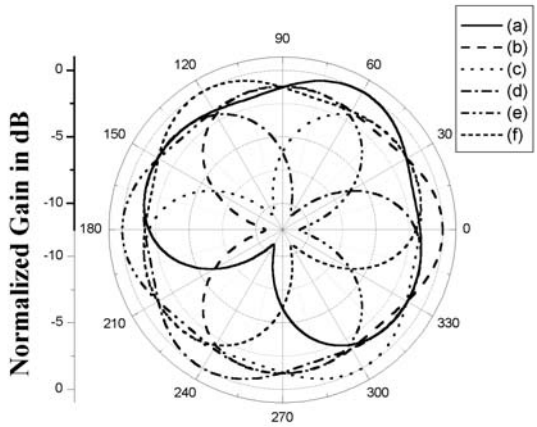

Fig. 8. Beam patterns (a) to (f) in the Azimuth Plane for Antenna Sampling Periods #1 to #6. Load Setting: $x_1 = 0\ \Omega$, $x_2 = 30\ \Omega$, $x_3 = 0\ \Omega$, $x_4 = 30\ \Omega$, $x_5 = 30\ \Omega$, $x_6 = 30\ \Omega$.

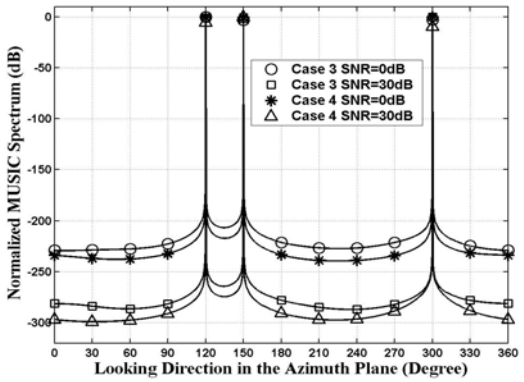

Fig. 9. MUSIC spectra for Cases 3 and 4 in different SNR environments. Load settings are listed in Table II. Signal directions: 120°, 150° and 300° in the azimuth plane.

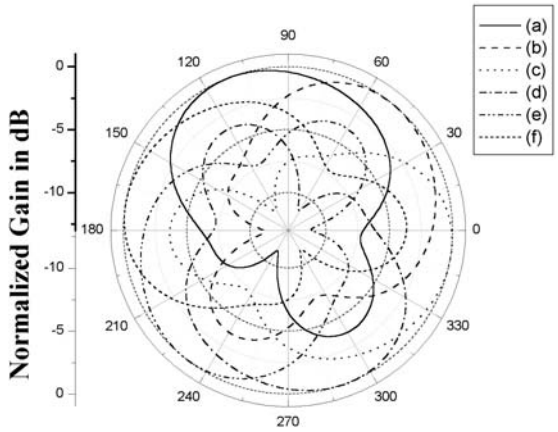

Fig. 10. Beam Patterns (a) to (f) in the Azimuth Plane for Antenna Sampling Periods #1 to #6. Load Reactance: $x_1 = 0\ \Omega$, $x_2 = 10\ \Omega$, $x_3 = 0\ \Omega$, $x_4 = -30\ \Omega$, $x_5 = 70\ \Omega$, $x_6 = 30\ \Omega$.

symmetric, the DOA can be estimated correctly. However, the load setting, which gives deep nulls in radiation patterns in any direction, should be avoided for the DOA estimation. Because signals coming from that region are received with low power

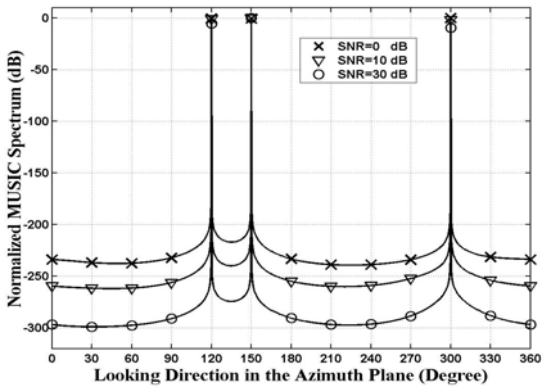

Fig. 11. MUSIC Spectra in Different SNRs Signal Environments. Signal Directions: 120°, 150° and 300° in the Azimuth Plane. Load Setting is Same as in Case 4.

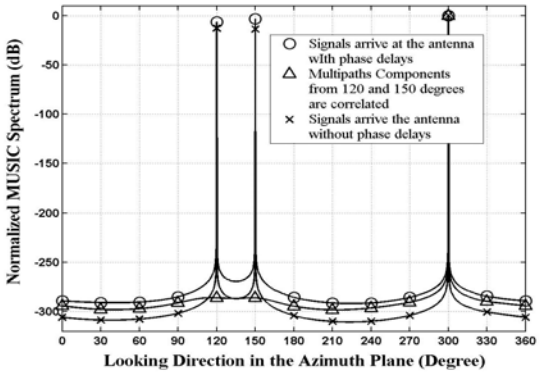

Fig. 12. MUSIC Spectra. Load Setting is Same as for Case 4. SNR = 30 dB. Signal Directions: 120°, 150° and 300° in the Azimuth Plane.

levels, or even be nulled out. Consequently, the DOA information of signal in this null region can not be resolved.

B. Performance in Different SNRs Environments

We simulate MUSIC spectra in signal environments with different SNRs. Suppose that signal sources are totally uncorrelated and have equal power. The individual SNR for each signal source is equally set. MUSIC spectra with 3 different SNRs from 0 dB to 30 dB are shown in Fig. 11. The figure shows that the performance of our proposed MUSIC algorithm degrades as SNR decreases, but three MUSIC spectra reach nearly the same peak values at signal directions.

C. Performance in a Multipath Propagation Environment

Our study assumes line-of-sight (LOS) propagations (Ricean channel). In a macroscopic environment, where PL services such as intelligent transportation services is employed, antennas are mounted well above the roof of the buildings to provide LOS propagations between base stations and mobile terminals [24].

Ideally, signals arrive at the antenna without phase delays. The plotted MUSIC spectrum is shown in Fig. 12 with a "×" marked solid line. In a real wireless communication environment, multipath propagation delays of the signals are expected. Received signals are an ensemble of LOS components and mulitpath components from each of the

Open Science Index, Electronics and Communication Engineering Vol:1, No:11, 2007 publications.waset.org/8581.pdf

far-field signal source. Knowing that the LOS components are uncorrelated with the multipath components [25]; and that LOS components have much higher signal power level. We can still reasonably represent received signals at the antennas as a summation of these LOS components from different directions with phase differences induced by the propagation delays. Signal directions are set as 120°, 150° and 300° in the azimuth plane; The MUSIC spectrum for delayed signals is shown in Fig. 12 with a "O" marked solid curve. The signal direction information can be extracted.

In a microscopic environment, base station antennas are mounted below the rooftop level to confine the signal coverage into a small local area. [26] In this case, base stations are located in a rich scattering environment. There are no LOS components. Signals received at the base station antenna are a collection of multipath components with angle spreads that are possible to be correlated. Fig. 12 shows the resulted MUSIC spectrum with a "Δ" marked solid line. Two multipath components from one far-field signal source arriving at the antenna from 120° and 150° in the azimuth plane are correlated. The MUSIC algorithm does not give the correlated signals' direction information. For the direction finding of coherent waves using a single RF-port ESPAR, a spatial smoothing technique has been developed for the antenna recently [27-29].

D. Resolution and Limitation in Number of Resolvable Signals

The proposed technique is capable to estimate the DOAs of two signal sources with 1° angular separation. As seen from Fig. 13, two signals from 149° and 150° in the azimuth plane are clearly resolved from the MUSIC spectrum. SNR is 30 dB.

The maximum number of uncorrelated waves can be estimated is M-1. M is the number of parasitic elements, the number of sampling periods and is also the dimension of the formed signal correlation matrix RUU. The scenario is similar to the conventional MUSIC algorithm, in which RUU with a dimension of M can produce up to M-1 signals [21, 30]. In our design, there are 6 parasitic monopoles, thus we can estimate up to 5 DOAs as shown in Fig.14. Signal directions are set to be: 60°, 100°, 120°, 180°, and 300° in azimuth plane.

E. Sampling Period and Periodicity of Transmitted Signals

Finally, we discuss the requirement of transmitted signals to be periodic when employing proposed technique for the DOA

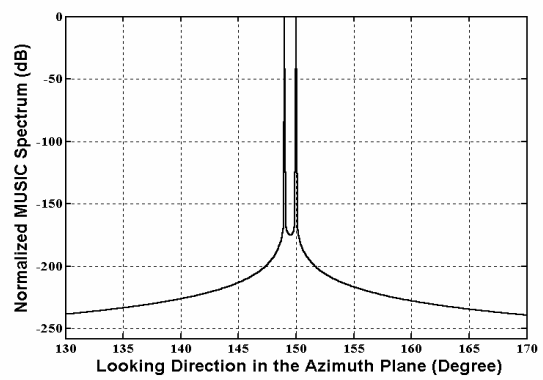

Fig. 13. MUSIC spectrum. Load Setting is Same as for Case 3. SNR=30 dB. Two Signal Directions Are 149°, and 150°, respectively, in the azimuth plane.

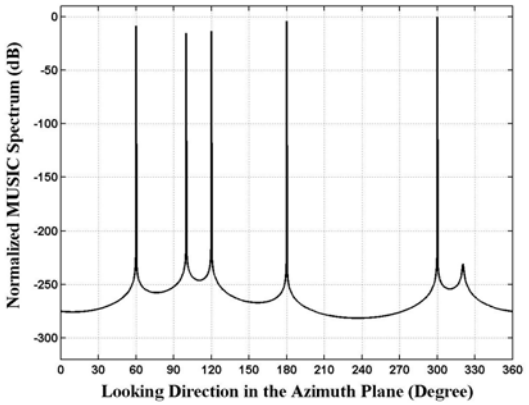

Fig. 14. MUSIC Spectrum. Load Setting is Same as for Case 3. SNR=30 dB. Signal Directions: 60°, 100°, 120°, 180°, and 300° in the Azimuth Plane.

estimation. In the derivation of $\mathbf{R}_{UU}$, we require that each individual signal source transmit periodic signals. In a practical wireless communication environment, time offsets among periodic signals and the antenna sampling periods, induced by different propagation path delays, are expected.

However, the signal period does not need to be aligned with the sampling period. (cf. Fig. 15) This is true because the signal source transmits a length of periodic signals longer than the length of total 6 sampling periods; and each signal period is the same as the antenna sampling period T. The received signals at the antenna are still periodic and (20) is therefore valid.

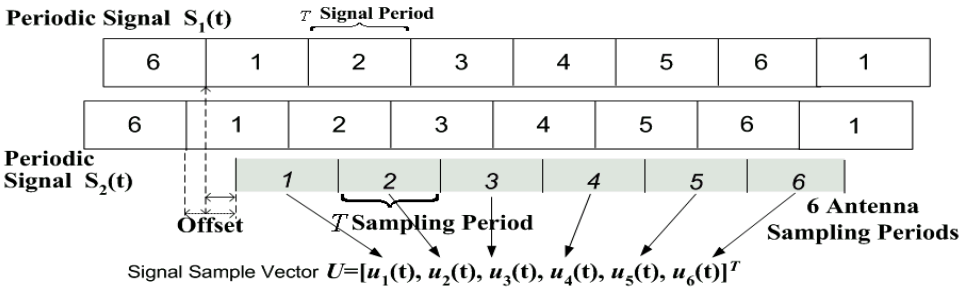

Fig. 15. Periodic Signal Time Slots, and Antenna Virtual Sampling Periods in the Proposed DOA Estimation Technique. Each Signal Contains 6 slots. The Antenna Rotates Six Times. Time Offsets are Expected in a Multipath Environment.

Open Science Index, Electronics and Communication Engineering Vol:1, No:11, 2007 publications.waset.org/8581.pdf

The requirement means that when doing DOA estimation, mobile terminals will transmit periodic signals instead of message signals. With the priori knowledge of the location of wireless base stations, where the antennas are mounted, and with the database of the map of the local area, PL service can be provided at the expense of a short message period. This is applicable in cases when mobile subscribers are in dangerous situations and need to make a rescue calls, such as the E999 call in Singapore and the E911 call in America.

F. Speed of DOA Estimation

In our design, 16 signal bits are stored at each sampling period. A minimum length of $16 \times 6 = 96$ bits of periodic signals for six antenna sampling periods is required. For Time Division Multiple Access System (TDMA IS-136), one frame comprises six time slots with a time length of 6.67 ms each. In each time slot, 260 data bits are transmitted. The tuning of the reactance can be accomplished in nanoseconds [22]. These indicate that the DOA estimation is possible to be carried out within less than one TDMA time slot.

V. Conclusion

In this paper a novel approach for executing high resolution MUSIC algorithm based on a single RF port smart antenna has been proposed. After presenting the configuration and the working principle of the antenna, the performance of the proposed technique for various aspects have been studied. The results have justified that the technique for a high-resolution DOA estimation of 1 degree, which is as good as a conventional MUSIC algorithm. The proposed technique for DOA estimation based on a signal RF port parasitic antenna has many advantages over that on a DBF. They are:

1) Low power consumption and low complexity obtained from using the single port antenna. Therefore, this technique is highly applicable to commercial PL services. This is the most outstanding benefit of our proposed DOA estimation technique.
2) Contrary to the DOA estimation based on a DBF, the mutual coupling is utilized to steer the beam [12]. Thus the modified MUSIC algorithm is free from negative influences of mutual coupling between elements. In a DBF this influence has to be compensated for the enhancement of system performance in a high-resolution DOA estimation as studied in [31], [32].
3) High quality performances in low SNR signal environments. The performances in SNR = 0 dB environment are shown in Fig. 9 and Fig. 11.
4) The proposed technique is very flexible in operation. When all loading reactance at parasitic monopoles are tuned adaptively to the signal environment, the antenna functions as a smart directional antenna serving to reduce the channel interferences and improve the channel capacity. At this time an adaptive beam-forming algorithm needs to be executed at base-band DSP to control the reactive loadings to the parasitic monopoles.
5) Parasitic elements are arranged to form a circular array antenna. When used for DOA estimation, it give the signal direction information covering 360° in the azimuth plane.

Simulation studies have also pointed out that further improvements are needed to enhance system performances to make it more applicable to practical wireless communication systems. The areas of improvements are as follows:

1) The proposed technique works in an uncorrelated signal environment. New methods should explore signal sources' spatial signatures in a correlated signal environment for PL services.
2) The proposed antenna will not suffer from the negative influence from the mutual coupling between antenna elements. However, the calibration of the antenna aperture over DOA, frequency and temperature, weather environment, and fabrication error is, however, still unavoidable [1] and they influence the antenna performances.
3) The Doppler effect of the fast moving mobile terminals needs to be investigated. The will benefit the application of the antennas on moving terminals.

Finally, the state-of-the-art wireless PL service is still a new area. New direction finding technologies that avail the realization of PL services are under investigation. This paper offers an economical approach to implement smart antennas into the existing terrestrial wireless mobile communications system, especially at the base stations to serve as an essential and fundamental technique of PL services.

References

[1] T. S. Rappaport, J. H. Reed and B. D. Woerner, "Position Location Using Wireless Communications on Highways of the Future," *IEEE Comms. Mag.*, Oct. 1996, pp. 33-41.

[2] K. J. Krizman, T. E. Biedka and T. S. Rappaport, "Wireless Position Location: Fundamentals, Implementation Strategies, and Sources of Error," *IEEE Vehicular Technology Conf.*, May 5-7, 1997, pp. 919-923.

[3] G. V. Tsoulos, "Smart antennas for mobile communication systems: benefits and challenges," *Elect. & Comm. Engg. J.*, Vol. 11, NO. 2, Apr. 1999, pp. 84 –94.

[4] J. C. Liberti, Jr. and T. S. Rappaport, *Smart Antennas for Wireless Communications: IS-95 and Third Generation CDMA Application*, Prentice Hall PTR, 1999.

[5] L. C. Godara, "Application of antenna arrays to mobile communications. II. Beam-forming and direction-of-arrival considerations," *Proc. IEEE*, Vol. 85 NO. 8, Aug. 1997, pp. 1195-1245.

[6] T. Ohira and J. Cheng, "Analog smart antennas", *Adaptive Antenna Arrays*, pp.184-204, ISBN3-540-20199-8, Berlin: Springer Verlag, June 2004.

[7] D. V. Thiel and S. Smith, *Switched Parasitic Antennas for Cellular Communications*, Artech House, 2002.

[8] S. L. Preston, D. V. Thiel, T. A. Smith, S. G. O'Keefe and J. W. Lu, "Base-station tracking in mobile communications using a switched parasitic antenna," *IEEE Trans. Antennas Propagat.*, Vol. 46, NO. 6, Jun. 1998, pp. 841 –844.

[9] R. Vaughan, "Switched parasitic elements for antenna diversity," *IEEE Trans. Antennas Propagat.*, Vol. 47, NO.2, Feb. 1999, pp. 399 –405.

[10] D. V. Thiel, S. G. O'Keefe and J. W. Lu, "Electronic beam steering in wire and patch antenna systems using switched parasitic elements," *IEEE Antenna Propagat. Symp. Dig.*, Vol. 1, 1996, pp. 534 –537.

[11] S. L. Preston, D. V. Thiel, J. W. Lu, S. G. O'Keefe and T. S. Bird, "Electronic beam steering using switched parasitic patch elements," *Elect. Lett.*, Vol. 33, NO. 1, 2 Jan. 1997, pp. 7 –8.

[12] R. F. Harrington, "Reactively controlled directive arrays," *IEEE Trans. Antennas Propagat.*, vol. AP-26, No.3, Mar. 1978, pp.390-395.

[13] T. Ohira and K. Gyoda, "Hand-held microwave direction-of-arrival finder based on varactor-tuned analog aerial beamforming," *Asia-Pacific Microwave Conf.*, 2001, pp. 585 –588.
[14] K. Yang and T. Ohira, "ESPAR antennas-based signal processing for DS-CDMA signal waveforms in ad hoc Network systems," *IEEE 3rd Workshop on Signal Proc. Adv. Wireless Comms.*, 2001. (SPAWC '01), 2001, pp. 130 –133.
[15] J. Cheng, Y. Kamiya and T. Ohira, "Adaptive Beamforming of ESPAR Antenna Based on Steepest Gradient Algorithm," *IEICE Trans. Comms.*, Vol.E84-B, No.7, 2001, pp.1790-1800.
[16] A. Komatsuzaki, S. Saito, K. Gyoda and T. Ohira, "Hamiltonian approach to reactance optimization in ESPAR antennas," *Asia-Pacific Microwave Conf. 2000*, Sydney, Australia, pp. 1514 –1517.
[17] C. Sun, A. Hirata, T. Ohira, and N. C. Karmakar, "Fast beamforming of electronically steerable parasitic array radiator antennas: Theory and experiment," *IEEE Trans. on Antennas and Propagat.*, vol. 52, no. 7, pp. 1819-1832, July 2004.
[18] S. A. Leonov and A. I. Leonov, *Handbook of Computer Simulation in Radio Engineering, Communications, and Radar*, Artech House, 2001, pp.175-176.
[19] C. A. Balanis, *Antenna theory Analysis and Design*, John Wiley. 1997.
[20] S. Y. Liao, *Microwave Solid-State Devices*, Printice Hall, 1985.
[21] R. O. Schmidt, "Multiple Emitter Location and Signal Parameter Estimation", *IEEE Trans. Antennas Propagat*., vol.AP-34, No.3, Mar. 1986, pp.276-280.
[22] D. H. Johnson and D. E. Dudgeon, *Array Signal Processing: Concepts and Techniques*, Prentice Hall PTR. 1993.
[23] D. C. Cox, R. R. Murray, H. W. Arnold, A. W. Norris and M. F. Wazowicz, "Cross-polarization coupling measured for 800 MHz radio transmission in and around houses and large buildings," *IEEE Trans. Antennas Propagat.*, vol. AP-34, No.1, Jan. 1986, pp.83-87.
[24] W. C. Jakes, *Microwave Mobile Communications*. New York: IEEE Press 1994.
[25] C. Tepedelenlioglu, *Modeling and Mitigation of Time-Selective and Frequency-Selective Fading in Single-Carrier and Multi-Carrier Communications*, Ph.D thesis, Univ. of Minnesota, May, 2001
[26] J. Parsons. *The Mobile Radio Propagation Channel*, New York: Halsted, 1992.
[27] A. Hirata, T. Aono, H. Yamada, and T. Ohira, "Reactance-domain SSP MUSIC for an ESPAR antenna to estimate the DOAs of coherent waves", *International Symp. Wireless Personal Multimedia Communications*, WPMC2003, 3, pp.242-246, Yokosuka, Oct. 2003.
[28] A. Hirata, E. Taillefer, T. Aono, H. Yamada, and T. Ohira, "Correlation suppression performance for coherent signals in RD-SSP-MUSIC with a 7-element ESPAR antenna", *European Conf. Wireless Tech., ECWT2004*, Amsterdam, Oct. 2004.
[29] E. Taillefer, E. Chu, and T. Ohira, "ESPRIT algorithm for a seven-element regular-hexagonal shaped ESPAR", *European Conf. Wireless Tech.*, ECWT2004, Amsterdam, Oct. 2004.
[30] R. O. Schmidt and R. E. Franks, "Multiple Source DF Signal Processing: An Experimental System," *IEEE Trans. Antennas Propagat.*, vol. AP-34, No.3, Mar. 1986, pp.281-290.
[31] Y. Inoue, K. Mori and H. Arai, "DOA error estimation using 2.6GHz DBF array antenna**"** *Asia-Pacific Microwave Conf.* 2001, pp. 701 –704.
[32] K. R. Dandekar, H. Ling and G. Xu, "Effect of mutual coupling on direction finding in smart antenna applications" *Elect. Lett.*, Vol.36, Issue: 22, Oct. 2000, pp. 1889 –1891.

Chen Sun completed the Ph.D. study at Nanyang Technological University, Singapore, in July 2004. He is now a researcher at ATR Wave Engineering Laboratories, Kyoto, Japan. From November 2002 to March 2003, he was a student intern with ATR Adaptive Communications Research Laboratories, Kyoto, Japan, working on personal wireless links for wireless ad hoc networks. His research interests include array signal processing, diversity combining techniques, MIMO communications and array antenna design. He was an invited session (Active and Adaptive Array Antennas) cochair in Asia-Pacific Microwave Conference 2002, Kyoto, Japan. He has published one book chapter, three international referred journal papers and many conference proceedings.

Nemai C. Karmakar obtained his M.S. and Ph.D. in electrical engineering from the University of Saskatchewan, Canada, and University of Queensland, Australia in 1991 and 1999, respectively. In August 1990, he was as a Research Assistant at the Communications Research Group, the University of Saskatchewan. From 1992 to 1995 he worked as a Microwave Design Engineer at Mitec Ltd., Australia, where he contributed significantly to the development of land mobile satellite antennas for the Australian Mobilesat. He taught at Queensland University of Technology, Australia in 1995–1996. From September 1998 to March 1999 he worked as a research engineer within the Radar Laboratory, Nanyang Technological University, Singapore. Since March 1999 he is an Assistant Professor and Graduate Advisor in the Division of Communications, the School of Electrical and Electronic Engineering, Nanyang Technological University, Singapore. He has published more than 100 referred journal and conference papers and three book chapters. He is a senior member of IEEE. He served as a member of the executive committee of Singapore IEEE Section in 2000 and is now an executive committee member of IEEE APS/MTT Chapter. He is a Senior Lecturer in the Department of Electrical and Computer Systems Engineering, Monash University, Clayton Campus, Monash, Australia.

Open Science Index, Electronics and Communication Engineering Vol:1, No:11, 2007 publications.waset.org/8581.pdf